# Complex spatiotemporal patterns in an open-flow reactor

Massimo Sangalli and Hsueh-Chia Chang*
*Department of Chemical Engineering, University of Notre Dame, Notre Dame, Indiana 46556*
(Received 3 June 1993; revised manuscript received 16 March 1994)

Reaction-diffusion systems in open-flow heterogeneous reactors are known to yield different instabilities and exhibit complex spatiotemporal dynamics. A particular mechanism leading to such behaviors is suggested here. Differential convection and differential diffusion can simultaneously induce instabilities at separate bands of wave numbers in an extended system where an activator-inhibitor reaction is taking place. The nonlinear interaction of these modes is shown to generate complex patterns with two different characteristic wavelengths and irregular temporal behavior in a distributed reactor for conditions at which a well-mixed reactor would exhibit no instability. The regions in the parameter space for two model kinetics where such patterns should exist are predicted *a priori* by normal form analysis of the relevant amplitude equations and validated with numerical simulations of the full partial differential equations. This mechanism for complex spatiotemporal behavior in open-flow reactors is expected to exist for many chemical reactions, including nonisothermal ones.

PACS number(s): 47.20.Ky, 47.54.+r, 82.40.Bj, 82.40.Ck

## I. INTRODUCTION

Spatially inhomogeneous patterns and irregular chemical oscillations are examples of complex spatiotemporal behavior exhibited by reaction-diffusion systems. The homogeneous steady state of a class of reactions, the activator-inhibitor systems, is known to exhibit more than one mode of instability. In addition to spatially homogeneous oscillations due to kinetic instability, spatially inhomogeneous patterns can be excited in such systems when the two species are not free to "move" with the same velocity along the reacting medium. Turing [1] was the first to show how a difference in the diffusivities of activator and inhibitor can destabilize the homogeneous steady state, resulting in a spatially inhomogeneous steady pattern. Almost four decades passed before a successful experimental confirmation of Turing's prediction was achieved [2]. This has spurred new interest in this nonequilibrium phenomenon induced by a coupling between diffusion and kinetics. Recently, Rovinsky and Menzinger [3] showed how such homogeneous steady states of activator-inhibitor systems can also be destabilized by a difference $\Delta v$ in the convective velocities of the two species. The resulting "convective" instability produces a traveling wave, which was soon obtained experimentally using a cation exchanger that immobilizes one of the two species [4]. While the Turing instability can take place only if the activator diffuses slower than the inhibitor, the convective instability can arise whenever there is a difference in the convective velocities, thus making the differential-convection-induced instability easier to observe than the Turing one.

In general, if the reaction is placed in an open-flow heterogeneous reactor, the different affinity of the species for the phases results in different effective convective velocities, an effect which is used for separation purposes in chromatographs. In fact, the possibility of inciting instability by differential transport in an open-flow reactor has important implications for a far larger class of reaction systems than those that exhibit isothermal chemical instability. For example, activator-inhibitor kinetics are encountered in nonisothermal reaction systems, where an exothermic reaction with sensitive Arrhenius type temperature dependence can cause the temperature to act as the activator, while a reactant may act as the inhibitor. (Increasing the temperature increases the temperature "production rate," while increasing the reactant concentration increases the reactant consumption rate.) Due to the difference in effective thermal and mass transport properties in an open-flow heterogeneous reactor, the same linear instabilities found in isothermal activator-inhibitor systems are expected to be common also in nonisothermal systems with simple kinetics. Indeed, thermal traveling waves and regular patterns have been reported in numerous studies, for example, in the latest experiments by Lane and Luss [5], who clearly demonstrated the existence of periodic thermal traveling waves, which could be due to a differential-transport-induced instability.

More complex spatiotemporal patterns are often observed in heterogeneous chemical reactors [6,7], but they cannot be understood with simple linear stability theory. A route to complexity commonly encountered in hydrodynamical systems involves the nonlinear interaction of modes with different wave numbers. The existence of multiple instabilities, such as the convective and Turing instabilities, immediately suggests the possibility of also generating complex spatiotemporal patterns due to this mechanism in chemical systems. A reasonable approach is to seek small-amplitude waves generated by weakly nonlinear interaction between two nearly neutral modes. Guckenheimer [8] investigated the interaction of a steady

*Author to whom all correspondence should be addressed.

 

Turing mode and a traveling wave whose wave number is determined by the system size and suggested the existence of a heteroclinic orbit for the Brusselator model and hence the possibility of chaotic behavior. Different results were obtained recently by Rovinsky and Menzinger [9] who studied the interaction of a homogeneous oscillatory kinetic instability, allowed by their no-flux boundary conditions, and the Turing mode. They concluded that a stable mixed mode (and the complex dynamics expected from its destabilization) does not exist in a one-dimensional reactor for a few model kinetics, including the Brusselator model. A mixed mode generated by such Hopf-Turing interaction would have only one characteristic wavelength, the one corresponding to the Turing instability.

In this paper we demonstrate that in the presence of differential convection and differential diffusion, the interaction between a short-wave modified Turing mode and a convective long-wave mode can generate mixed-mode waves with two distinct characteristic length scales and even irregular waves with chaotic temporal patterns. The possibility of this more complex spatiotemporal behavior occurs at low differential convective velocity $\Delta v$ for which we show that differential diffusion and differential convection can act separately at different characteristic length scales to destabilize the system. A codimension-2 singularity exists when a modified Turing mode at wave number $k_B \sim k_T$, where $k_T$ is the Turing wave number, and a convective mode at small wave number $k_A \sim O(\Delta v/\sqrt{K/D_2})$, where $\Delta v$ is the differential convective velocity between the activator and the inhibitor, $K$ is a characteristic rate constant for their reaction, and $D_2$ is the diffusivity of the inhibitor, become neutrally stable for the same kinetic parameters. With a small but finite $\Delta v$, both instabilities are of the Hopf variety which gives rise to traveling waves. Interestingly, the interaction of these waves in a distributed system generates very complex behavior for conditions in which a well-mixed reactor does not exhibit oscillations, viz., the homogeneous kinetics is linearly stable. As $\Delta v$ approaches zero, $k_A$ vanishes and the convective mode approaches the homogeneous oscillatory kinetic mode, while the short-wave mode becomes the Turing static instability. We show that the complex wave dynamics still survives in this limit although the convective length scale, and with it some of the spatial complexity, is lost from the pattern. This limiting result, which is in contrast with that of Rovinsky and Menzinger [9], is confirmed with numerical integration. Different from the finite differential convection case, linear oscillatory instability of the well-mixed system is necessary in this limit in order to observe the complex behavior in the distributed system. At large $\Delta v$ the characteristic wavelengths of the two instabilities at the singularity become indistinguishable, resulting in a single traveling wave which is qualitatively identical to the one studied both theoretically and experimentally by Rovinsky and Menzinger [3,4] in the presence of the convective instability only. Consequently, the complex wave patterns due to our short-long wave interaction mechanism only occur for small but finite differential velocities, a condition that is generally satisfied in a chromatograph or a heterogeneous reactor if the reactants have approximately the same affinity for the solid phase. We study this interesting region by deriving leading order estimates for the wave numbers of the two instabilities and locating the singular loci in the parameter space where both modes are neutrally stable. These loci correspond to a double-Hopf singularity for finite $\Delta v$ and approach a pitchfork-Hopf singularity for vanishing $\Delta v$. High codimension bifurcation theory is then applied to derive the relevant amplitude equations valid in the neighborhood of the loci and to investigate, through normal form analysis, the existence of stable mixed modes and heteroclinic orbits. We finally validate the resulting *a priori* predictions of the loci of secondary bifurcations to such complex wave patterns for some model inhibitor-activator kinetics with a numerical analysis of the full equations.

## II. THE EXISTENCE OF TWO COMPETING MODES

Consider the mass balance equations for a two-species reaction-diffusion system:

$$\begin{aligned} \frac{\partial c_1}{\partial t} + \mathbf{v}_1 \cdot \nabla c_1 &= f_1(c_1, c_2; \mathbf{r}) + D_1 \nabla^2 c_1 \ , \\ \frac{\partial c_2}{\partial t} + \mathbf{v}_2 \cdot \nabla c_2 &= f_2(c_1, c_2; \mathbf{r}) + D_2 \nabla^2 c_2 \ , \end{aligned} \tag{1}$$

where $f_1$ and $f_2$ contain the reaction kinetics which depend on the kinetic vector parameter $\mathbf{r}$. The transport parameters are the effective diffusivities $D_1$ and $D_2$ and the effective velocities $\mathbf{v}_1$ and $\mathbf{v}_2$. The pseudohomogeneous model of (1) may be obtained, for example, by averaging a complex heterogeneous system in which the chemical reactions take place in one of the phases and are absent or at equilibrium in the other phase. Hence the transport properties are effective in the sense that they may correspond not to the molecular values in a single phase, but to the proper average over the different phases in the heterogeneous reactor. For example, $\mathbf{v}_1$ and $\mathbf{v}_2$ can be effective convective velocities in a chromatograph, which can vary depending on the affinity of the two components for the substrate. In our analysis, we will restrict ourselves to one unbounded spatial dimension. In this case, we can always rescale the equation and carry out a moving coordinate transformation, corresponding to a Lagrangian frame moving at velocity $v_2$, to reduce the number of parameters, yielding

$$\frac{\partial \mathbf{c}}{\partial t} = \mathbf{f}(\mathbf{c}) + \mathbf{D}\frac{\partial^2 \mathbf{c}}{\partial \xi^2} + \mathbf{V}\frac{\partial \mathbf{c}}{\partial \xi} \ , \tag{2}$$

where

$$\mathbf{c} = \begin{bmatrix} c_1 \\ c_2 \end{bmatrix}, \quad \mathbf{f} = \begin{bmatrix} f_1 \\ f_2 \end{bmatrix}, \quad \mathbf{D} = \begin{bmatrix} \delta & 0 \\ 0 & 1 \end{bmatrix},$$

$$\mathbf{V} = \begin{bmatrix} v & 0 \\ 0 & 0 \end{bmatrix}, \quad \delta = \frac{D_1}{D_2}, \quad v = v_2 - v_1 \ .$$

In (2), scaling by the characteristic length $\sqrt{D_2/K}$ and time scale $1/K$ has been carried out so that the normal-

ized diffusivity of the second species is unity exactly. The reaction rates $f_i$ and the components of the velocities in the $\xi$ direction $v_i$ also correspond to the original ones scaled by $K$ and $\sqrt{KD_2}$, respectively.

The linear stability of the homogeneous steady state $\mathbf{c}_0$, which satisfies $\mathbf{f}(\mathbf{c}_0)=0$, will depend on the eigenvalue problem obtained by linearizing (2) around $\mathbf{c}_0$. For an unbounded system the problem is translationally invariant which allows a normal mode expansion of the vector of deviation variables $\mathbf{c}'=\mathbf{c}-\mathbf{c}_0$ of the type

$$\mathbf{c}'=\mathbf{x}\exp(-ik\xi+\lambda t) .$$

The relevant eigenvalue problem will then be $\mathbf{J}\mathbf{x}=\lambda\mathbf{x}$ and the Jacobian $\mathbf{J}$ will have the form

$$\mathbf{J}=\mathbf{A}-k^2\mathbf{D}-ik\mathbf{V} , \tag{3}$$

where

$$\mathbf{A}=\begin{bmatrix} a_{11} & a_{12} \\ a_{21} & a_{22} \end{bmatrix}$$

represents the linearized kinetics governing the stability to homogeneous perturbations. We shall show here that two linear instabilities can coexist for small $v$ such that the growth rate associated with the real part of the more unstable eigenvalue of $\mathbf{J}$,

$$\lambda_R=\frac{a_{11}+a_{22}-(\delta+1)k^2+[\frac{1}{2}(q^2+p^2)^{1/2}+\frac{1}{2}q]^{1/2}}{2} , \tag{4}$$

where

$$q=[a_{11}-a_{22}-(\delta-1)k^2]^2+4a_{12}a_{21}-k^2v^2$$

and

$$p=2vk[a_{11}-a_{22}-(\delta-1)k^2] ,$$

can exhibit two maxima as a function of the wave number $k$. This will happen both in the Turing-Hopf case, where there is no difference in the convective velocities (i.e., $v=0$), in which case the two critical modes are spatially homogeneous oscillation and a steady (in the moving frame of reference) Turing mode, and when there is a difference in convective velocities which leads to two traveling wave instabilities (see Fig. 1).

The region where the differential convection is small can be conveniently studied with a perturbative formulation of the eigenvalue problem. The Jacobian is written $\mathbf{J}=\mathbf{J}_0+v\mathbf{J}_1$, where $\mathbf{J}_0=\mathbf{A}-k^2\mathbf{D}$ and

$$\mathbf{J}_1=\begin{bmatrix} -ik & 0 \\ 0 & 0 \end{bmatrix} ,$$

and letting $\lambda=\lambda_0+v\lambda_1+O(v^2)$, $\mathbf{x}=\mathbf{x}_0+v\mathbf{x}_1+O(v^2)$, we can sequentially solve for the successive corrections to the eigenvalues $\lambda_i$ and eigenvectors $\mathbf{x}_i$ by using the Fredholm alternative technique for spectral perturbation.

At zeroth order, i.e., in the absence of differential convection, the eigenvalue problem is $\mathbf{J}_0\mathbf{x}_0=\lambda_0\mathbf{x}_0$. We recover in this case the previously studied [9] Hopf-Turing singularity. The singularity exists if there is an intersection in the parameter space between the loci $H_0$ and $T_0$ at which an oscillatory (Hopf) homogeneous mode and an inhomogeneous Turing mode with wave number $k_T$, respectively, become critical. These loci and the critical wave number $k_T$ have the following expressions:

$$(H_0):\ \mathrm{tr}(\mathbf{A})=a_{11}+a_{22}=0 , \tag{5a}$$

$$(T_0):\ a_{11}a_{22}-a_{12}a_{21}-\frac{(a_{11}+a_{22}\delta)^2}{4\delta}=0 , \tag{5b}$$

$$k_T^2=\frac{a_{11}+a_{22}\delta}{2\delta} , \tag{5c}$$

from which it can be seen that for the Turing mode to coexist at criticality with an oscillatory homogeneous neutral mode, we need to have $a_{11}$ and $a_{22}$ of opposite sign, i.e., an activator-inhibitor system, and the diffusivity of the activator smaller than that of the inhibitor. In the remainder of the paper, we will assume these conditions to be satisfied. In particular, we will stipulate $a_{11}>0$ and

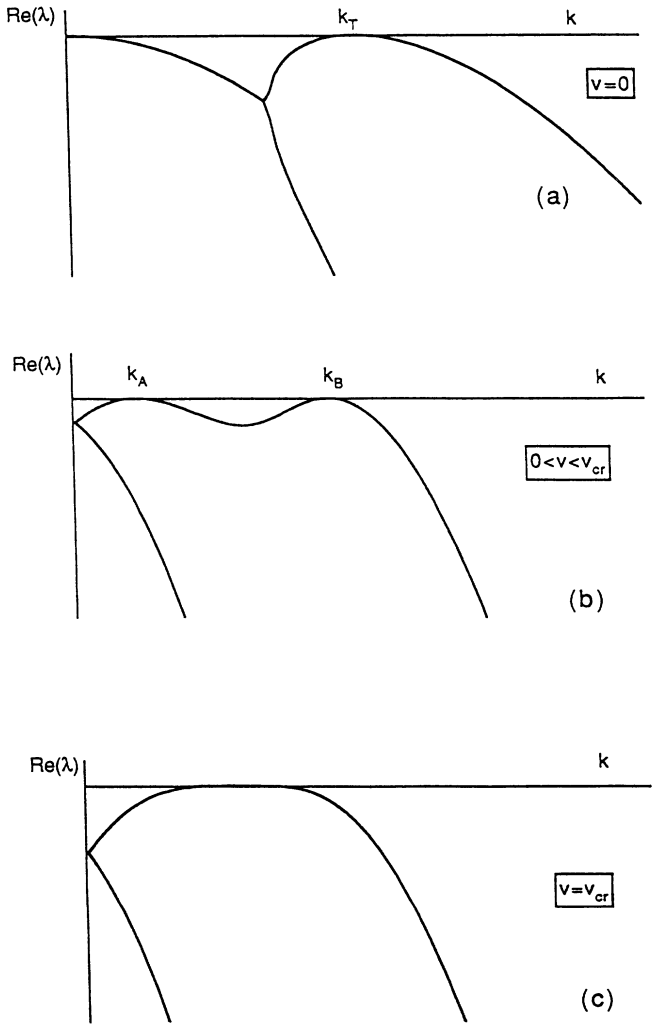


FIG. 1. Growth rate vs wave number at the codimension-2 singularity for different values of the differential velocity $v$.

$a_{22}<0$, viz., $c_1$ is the concentration of the activator and $c_2$ that of the inhibitor, and accordingly $\delta<1$. At the intersection locus we will have a $(0,\pm i\omega_0)$ singularity at which the eigenvalues of $\mathbf{J}_0$ will be purely imaginary with frequency $\omega_0$ at $k=0$, complex conjugate at low $k$, and branching into two real modes at higher wave numbers, the more unstable of which will lead to the Turing critical mode, as shown in Fig. 1(a).

At first order in $v$, we can obtain the effect of the presence of a small differential velocity on the locus and type of the singularity. We are primarily interested in the correction $\lambda_1$ to the eigenvalues. Its general expression is

$$\lambda_1=\frac{\langle \mathbf{J}_1\mathbf{x}_0,\hat{\mathbf{x}}_0\rangle}{\langle \mathbf{x}_0,\hat{\mathbf{x}}_0\rangle}\ , \tag{6}$$

where $\hat{\mathbf{x}}_0$ is the adjoint eigenvector for the zeroth order eigenvalue problem and $\langle\ ,\ \rangle$ is the Euclidean inner product for complex vectors. For parameters close to the ones yielding the Hopf-Turing singularity and for small enough $k$, $\mathbf{x}_0$ and $\hat{\mathbf{x}}_0$ are complex, so that (6) yields in general a complex $\lambda_1$ with nonzero real part. When $v\neq 0$, the two eigenvalues for small $k$ have therefore different real parts for $k\neq 0$, and the most unstable of the two growth rates can exhibit a maximum at a wave number having an order $v$ deviation from zero. We can consequently use, for small $v$, a long wavelength expansion of the growth rate (4):

$$\lambda_R\cong\frac{(a_{11}+a_{22})}{2}+\frac{(a_{11}-a_{22})|v|}{2[-(a_{11}-a_{22})^2-4a_{12}a_{21}]^{1/2}}k -\frac{\delta+1}{2}k^2+O(k^3) \tag{7}$$

to obtain the following first order estimates for the modified locus $H_1$ and the critical wave number $k_A$ of this bifurcation to a long-wave convective mode:

$$(H_1):\ (a_{11}+a_{22})+k_A^2(\delta+1)=0\ , \tag{8a}$$

$$k_A=\frac{(a_{11}-a_{22})|v|}{2[-(a_{11}-a_{22})^2-4a_{12}a_{21}]^{1/2}(\delta+1)}\ . \tag{8b}$$

Equation (8a) implies that in the presence of a nonzero differential velocity, the homogeneous kinetics are stable at criticality, while the critical wave number is shown from (8b) to be a linearly increasing function of the differential velocity to leading order. As $v$ tends to zero, the critical wave number $k_A$ vanishes and the locus $H_1$ tends to $H_0$. The critical frequency is $\omega_A=\omega_0+O(v)$, so that in general we will have for small $v$ a long traveling wave mode due to the interaction between differential convection and kinetics.

For $k\sim k_T$ at the short-wave Turing mode, the eigenvector $\mathbf{x}_0$ and the adjoint eigenvector $\hat{\mathbf{x}}_0$ are real. Since $\mathbf{J}_1$ is purely imaginary, (6) implies that $\lambda_1$ will be so also. Therefore, there will be *no* $O(v)$ correction to the growth rate $\mathrm{Re}(\lambda_0)$ of the short-wave mode, yielding to this order the same locus $T_0$ of the Turing bifurcation. However, the critical eigenvalue will now have a nonzero $[O(v)]$ imaginary part, so that $T_0$ will now be a bifurcation locus for a traveling wave with $O(v)$ phase speed. In general, it will still be possible to find an intersection between $T_0$ and $H_1$ so that both the long and short traveling waves will be neutrally stable, with a resulting growth rate depicted in Fig. 1(b). It is clear from the above $O(v)$ asymptotic analysis that the steady-Hopf $(0,\pm i\omega_0)$ singularity of the kinetic and Turing instabilities at $v=0$ is transformed into a Hopf-Hopf $(\pm i\omega_A,\pm i\omega_B)$ singularity of the convective and Turing instabilities at finite differential velocity. The introduction of an additional parameter $v$ into the reaction-diffusion system essentially enlarges the possibility of encountering a codimension-2 singularity. Alternatively, differential flow in an open-flow system promotes the potential appearance of complex wave patterns that will be shown to exist near these singularities.

The leading order effect of finite $v$ on the growth rate of the modified Turing mode can be found by solving the order $(v^2)$ problem. When $k_T>1$, this critical mode can be captured by the simpler short wave expansion of (4), which can be rewritten as

$$\mathrm{Re}(\lambda)=\mathrm{Re}(\lambda_0)+\frac{\chi v^2}{k^4}+O\left[\frac{1}{k^6}\right]\ .$$

For parameters close to the ones yielding the Turing-Hopf singularity,

$$\chi=\frac{(a_{11}-a_{22})^2-12a_{12}a_{21}}{4(1-\delta)^3}$$

is positive, implying that the leading order effect of a small but finite $v$ on the short-wave growth rate is a *quadratic* decrease from $k_T$ of the maximum-growing wave number with increasing $v$. This result, together with (8b), suggests that at increasing differential velocity the critical wave numbers at the singularity will move towards each other, as shown schematically in Fig. 1. At a limiting value of differential velocity $v_{\mathrm{cr}}$, the critical wave numbers will meet, as shown in Fig. 1(c), and the codimension-2 singularity will disappear. It can in fact be shown that when $v$ is sufficiently large, the growth rate exhibits only one maximum for positive wave numbers. The exact location of the critical velocity can be found tracing the singularity numerically, using (4) and solving the equations

$$\begin{aligned}\lambda_R(\mathbf{r},\delta,v,k_A)&=\frac{\partial\lambda_R}{\partial k}(\mathbf{r},\delta,v,k_A)=0\ ,\\ \lambda_R(\mathbf{r},\delta,v,k_B)&=\frac{\partial\lambda_R}{\partial k}(\mathbf{r},\delta,v,k_B)=0\end{aligned} \tag{9}$$

for $0\le k_A<k_B$. Above the limiting differential velocity $v_{\mathrm{cr}}$, at which $k_A=k_B$, only one critical traveling wave mode will be possible, with resulting behavior similar to the one described by Rovinsky and Menzinger [3]. Complex spatiotemporal dynamics can be expected before this limit, when a $(\pm i\omega_A,\pm i\omega_B)$ singularity exists, as shown in Fig. 1(b). We shall hence focus our effort to this interesting region where $\Delta v^2/D_2K$ is small.

## III. NORMAL FORM ANALYSIS CLOSE TO THE CODIMENSION-2 SINGULARITY

To study the nonlinear behavior for small values of $v$ near the codimension-2 singularity characterized by the double-hump growth rate of Figs. 1(a) and 1(b), we expand the solution in terms of the eigenfunctions at the singularity. Assuming that the neutral modes have amplitude of $O(|A|)$, and that all the other (stable) modes have amplitudes at least of $O(|A|^2)$ in this near-critical weakly nonlinear analysis, we only need to retain the discrete harmonics of the two neutral modes $k_A$ and $k_B$ (or 0 and $k_T$) and their sum and difference modes ($mk_A \pm nk_B$, where $m$ and $n$ are integers including zero). This assumption is only an approximation for an unbounded system characterized by a continuous spatial spectrum. It omits the possibility of interaction among neighboring "sideband" modes with arbitrarily close wave numbers and growth rates [10]. The possibility of complex behavior (e.g., phase turbulence) in reaction-diffusion systems due to such interaction is well known [11] and will not be tackled here. Another mechanism known to produce interesting dynamics but also omitted here is the subharmonic instability [12]. Hence, our interest in this paper is to study the possibility of complex behavior arising from interaction of nearly neutral modes close to a codimension-2 singularity. Near the singularity, this mechanism is expected to dominate the sideband and subharmonic instabilities but beyond it, the latter two may contribute to the complexity of the spatiotemporal behavior. With this in mind, we expand (2) in truncated Taylor series, retaining terms up to cubic order, and substitute for the deviation variables c' a discrete expansion in the selected linear eigenmodes. We then take an appropriate inner product with the adjoint eigenmodes to derive generic coupled amplitude equations. Center manifold theory is used to project the dynamics of the resulting system of ordinary differential equations (ODE's) on the two modes which are neutrally stable at the singularity. A nonlinear near-identity transformation can finally be used to eliminate all nonresonant quadratic and cubic terms in the amplitude equations. The details of this standard procedure, which are different for the double-Hopf and the steady-Hopf cases, are omitted here for the sake of brevity and can be found in the thesis of one of the authors [13]. In the absence of convection the procedure yields a pitchfork-Hopf normal form for the $(0, \pm i\omega_0)$ singularity—a result of the $Z_2$ symmetry of the reaction-diffusion system to translation and reflection.

Therefore, for both $v=0$ and $v \neq 0$, with the exception of the few discrete values of $v$ yielding resonance conditions, the local behavior close to the singularity is described by the unfolded normal form

$$\begin{aligned} \dot{r}_1 &= \mu_1 r_1 + \rho_1 r_1^3 + \rho_2 r_1 r_2^2 , \\ \dot{r}_2 &= \mu_2 r_2 + \rho_3 r_2^3 + \rho_4 r_2 r_1^2 \end{aligned} \tag{10}$$

governing the evolution in time of the real amplitudes $r_1$ and $r_2$ of the critical modes, which are to leading order decoupled from the relative phases. The unfolding parameters $\mu_1$ and $\mu_2$ are small deviations from zero of the real part of the eigenvalues of the critical modes resulting from a perturbation from the singularity in the parameter space.

The analysis of the planar system (10) for different possible combinations of $\mu_i$ and $\rho_i$ has been reported [14], and in the following only some of the results will be discussed in detail. In addition to the origin, up to three additional fixed points are possible, as shown in Fig. 2(a). The two critical modes can independently evolve into two finite-amplitude saturated pure-mode steady states ($F_1$ and $F_2$) corresponding to either homogeneous oscillations, periodic traveling waves, or a steady periodic pattern for the full system (1). Nonlinear interaction of the modes can give rise to more interesting behavior. The two pure-mode steady states can lose their stability through pitchfork bifurcations and a "mixed mode," a finite-amplitude steady-state combination of both modes [$F_3$ in Fig. 2(a)], can then appear. This fixed point, in turn, can lose its stability through a Hopf bifurcation and give rise to slow oscillations of the amplitudes. These periodic attractors can exist only when specific conditions on the normal form coefficients are satisfied, reducing the cases where the more complex dynamic behavior can occur to only two of the possible ones reported by Guckenheimer and Holmes [14]. One is their case VIIa, in which both modes have the same kind of bifurcation (soft or hard) at the singularity, and the other is case VIa, in

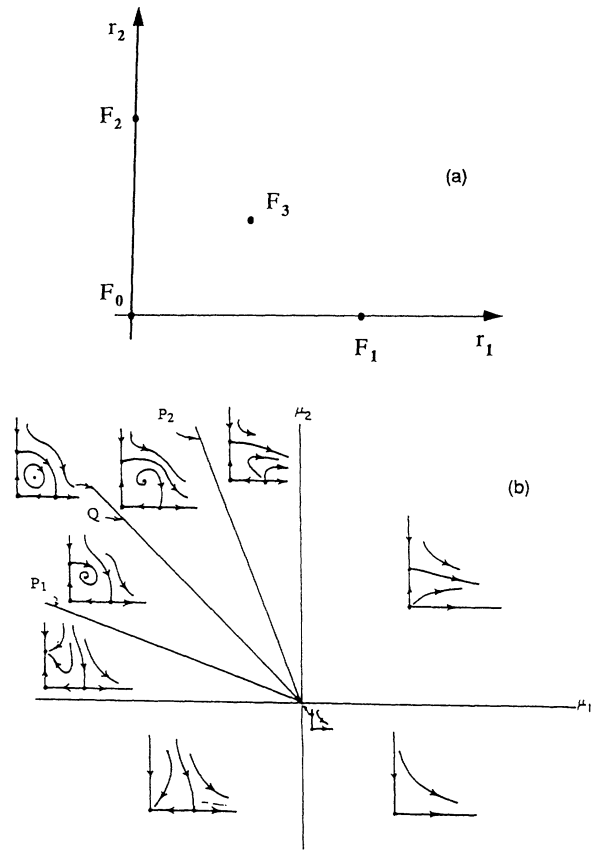


FIG. 2. (a) Possible fixed points for the planar system (10). (b) Partial bifurcation set and phase portraits for the unfolding of case VIa in Ref. [14].

which one of the neutral modes is subcritical and the other supercritical at the singularity. A possible combination of coefficients yielding the latter case is when $\rho_1$ and $\rho_2$ are positive, $\rho_3$ and $\rho_4$ are negative, and $\Delta=\rho_1\rho_3-\rho_2\rho_4$ is positive. In Fig. 2(b) the unfolding scenarios for this case, on which we will focus in the rest of the paper, are reproduced. The family of limit cycles resulting from the instability of the mixed mode can disappear in this case through an heteroclinic cycle connecting the three other steady states. The periodic and heteroclinic orbits appear together at line $Q$ under third order resolution of (10), and their relative location and stability cannot be ascertained without including higher order terms in the normal form.

These attractors for the planar system (10) correspond to complex wave patterns for the original system (1). The mixed mode, which is stable between $P_1$ and $Q$ in the unfolding of Fig. 2(b), corresponds to wave-packet-like nonstationary traveling waves with two wavelengths and two frequencies for the case with differential convection. Without convection, it corresponds to a nonhomogeneous pattern where all points oscillate in time with the same phase. The periodic orbits of the planar system appearing at line $Q$ correspond to patterns for the original system with one spatial characteristic length when $v=0$ and two when $v\neq 0$, oscillating in time with two characteristic frequencies if $v_1=v_2=0$, and three frequencies in presence of nonzero convection velocities. The heteroclinic orbit can yield a strange attractor near $Q$ due to a well-known entanglement mechanism [14]. Even in the absence of the strange attractor, chaotic transients are expected in such systems [15]. The pattern is expected to exhibit intermittent excitation of the two pure modes and the homogeneous steady state in time. In the fast transition period from one pure mode to the other, waves of two different wavelengths should appear on the medium. This is the richest wave pattern one expects from the interaction of the Turing and convective instabilities.

It should be noted that these patterns exist for conditions at which the origin fixed point (the homogeneous state) is stable to one instability but unstable to another. This has an important implication. It suggests that a system that is stable to the Turing instability can still produce complex wave patterns with the short Turing characteristic wavelength if it is unstable to the long-wave instability, i.e., the homogeneous oscillations resulting from unstable kinetics or the traveling wave resulting by the coupling of kinetics and differential convection, and if the nonlinear mechanism allows interaction between the supercritical long-wave mode and the subcritical Turing mode. This may allow the formation of Turing patterns in systems in which the linear instability is not possible because, for example, of the restrictions on the value of the diffusivities ratio (these include most exothermic systems, in which the diffusivity of the activator, i.e., the thermal diffusivity, is usually larger than the characteristic mass diffusivity). The convection hence enhances the possibility that the Turing structures may be observed.

The values of the normal form coefficients $\rho_i$ will depend, in general, on the kinetic parameters $\mathbf{r}$, the diffusivity ratio $\delta$, and the difference in convective velocities $v$. Given a kinetic model, the task will be to compute, along the locus of the singularities, the coefficients in (10) and check for the possibility of interesting behavior. The location of the different bifurcations that lead to complex wave patterns in the parameter space can then be obtained by computing the leading order (i.e., linear) relationships between $\mu_1,\mu_2$ and the original parameters. This will allow tracing of bifurcation loci such as $P_1$, $P_2$, and $Q$ in the original parameter space. Being singularities of codimension 2, two unfolding parameters will be needed. We hence have some freedom in choosing the two unfolding parameters while keeping the rest constant.

## IV. NORMAL FORM ANALYSIS AND SIMULATIONS IN THE BRUSSELATOR AND OREGONATOR MODELS

We will first illustrate the possibility of the nonlinear interactions described in Sec. III with a simple model known as the Brusselator [16], for which

$$\begin{aligned} f_1(c_1,c_2)&=a-(b+1)c_1+c_1^2c_2\ , \\ f_2(c_1,c_2)&=bc_1-c_1^2c_2\ . \end{aligned} \tag{11}$$

There are hence two kinetic parameters $a$ and $b$ and two transport parameters $v$ and $\delta$. The simplicity of this fictitious model allows some analytical results, such as an explicit expression of the locus of the Turing-Hopf singularity in the parameter space [11]. The linearization of (11) around the homogeneous steady state $\mathbf{c}_0=[a,b/a]^T$ yields $a_{11}=-1+b$, $a_{12}=a^2$, $a_{21}=-b$, and $a_{22}=-a^2$, and Eqs. (5a) and (5b), giving the loci $H_0$ and $T_0$, respectively, in the parameter space, become

$$b=\begin{cases} 1+a^2 & (H_0) \\ 1+\sqrt{\delta}a)^2 & (T_0)\ . \end{cases} \tag{12}$$

The Turing-Hopf singularity, the intersection of $T_0$ and $H_0$, is a line $\Gamma$ in the three-dimensional $(a,b,\delta)$ parameter space, whose projection on the $a$-$\delta$ plane is defined by $a=2[\sqrt{\delta}/(1-\delta)]$. Along $\Gamma$, we will have purely imaginary pairs of eigenvalues $\pm ia$ at $k=0$ and a zero eigenvalue at $k_T=\sqrt{2}/(1-\delta)$. Kuramoto [11] also showed that the oscillating homogeneous patterns bifurcating from $\Gamma$ are phase stable, viz., stable to the Eckhaus sideband instability, so that chaotic patterns due to the interaction of neighboring modes should not be observed and their omission in the present analysis is justifiable.

The normal form coefficients $\rho_i$ in (10) have been computed along the singular line $\Gamma$. The Hopf bifurcation is found to be always supercritical, in agreement with Kuramoto's results for the whole locus $H_0$. The other coefficients change sign along $\Gamma$ and the results are summarized in Fig. 3, where different symbols correspond to different unfolding scenarios depicted in Guckenheimer and Holmes [14]. The results show that complex behavior is possible for some values of the parameters. (A full picture can be obtained from our Fig. 3 and their unfoldings, in which their $r_1$ and $r_2$ correspond to the amplitude of our Turing mode and homogeneous oscilla-

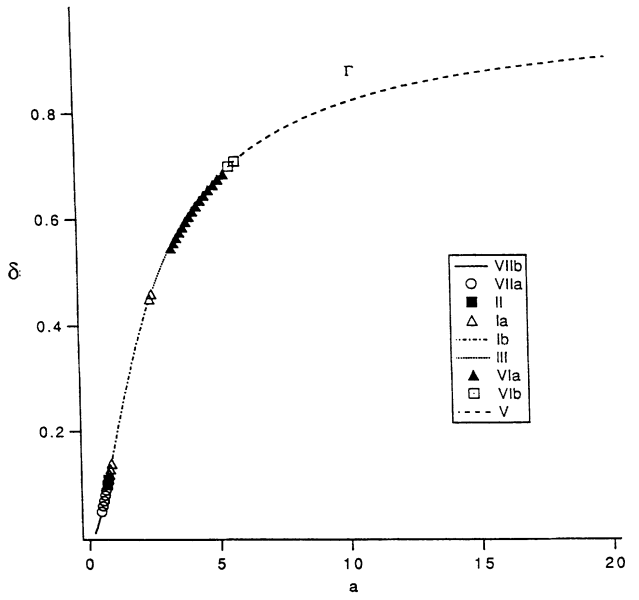


FIG. 3. The Turing-Hopf singularity line Γ in the Brusselator model. Different symbols correspond to different unfolding scenarios cases. See Ref. [14] for unfoldings of cases other than VIa.

tions, respectively.) In particular, there exists a range of parameters for which the system exhibits case VIa, whose unfolding scenario, including a stable mixed mode and the periodic-heteroclinic orbits, is shown in Fig. 2(b) and was discussed in Sec. III. The unfolding in the kinetic parameter space $(a,b)$ for one of the points of this case, the singularity at $\delta=0.5776$, is demonstrated in Fig. 4 in which lines $P_1$, $P_2$, and $Q$ correspond to lines with the

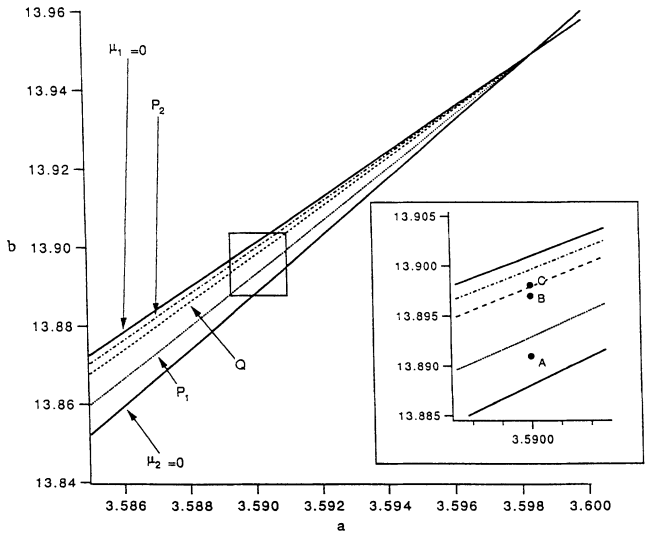


FIG. 4. The predicted unfolding in the kinetic parameters $a,b$ of the Brusselator model from the normal form analysis performed around the Hopf-Turing singularity with $\delta=0.5776$. The inset shows the points for which simulations are shown in Figs. 5 and 6.

same name in Fig. 2(b). We are now ready to predict the dynamics of (1) near the singularity for the case in which there is no differential convection. The line $\mu_2=0$, tangent to the curve in which the trace of the homogeneous Jacobian **A** vanishes, is the linear stability limit above which small perturbations of the homogeneous steady state will grow as homogeneous oscillations and saturate. The line $P_1$ separates finite-amplitude homogeneous oscillations from a mixed mode given by the superposition of homogeneous oscillations and either a steady inhomogeneous pattern (in the absence of convection velocities) or a traveling wave (if the two species are convected with the same velocity through the medium). The line $Q$ represents the loss of stability of this mixed mode to give rise to two- or three-tori depending again on the value of $v_1=v_2$, and a heteroclinic orbit around which complex spatiotemporal behavior is expected. Numerical simulations of the full partial differential equation (PDE) (1) with $v_1=v_2=0$, $D_1=\delta$, and $D_2=1$, in a finite domain large enough to contain four wavelengths of the critical Turing mode, are carried out to verify the predictions of the analysis which are different from the previous results of Rovinsky and Menzinger [9]. We adopt their no-flux boundary conditions, for which, in the absence of convection, the results of the normal form analysis are the same as those for an unbounded domain. The method of lines is used in the simulations, with fourth order finite differencing (second order at the boundaries) in space and a fourth order Runge-Kutta algorithm in time. Small random deviations from the homogeneous steady state were adopted as initial conditions. As is evident from the space-time patterns resulting after transient and reproduced in Figs. 5(a) and 5(b) for parameters corresponding, respectively, to points A and B in Fig. 4, the prediction of the bifurcation from the pure mode (homogeneous oscillations) to the mixed mode (saturated oscillating pattern with one characteristic wavelength) is found to be accurate. In Fig. 6 a time series of the concentration of the activator at the left boundary of the domain for parameters corresponding to point $C$ in Fig. 4 shows the predicted transition to a pattern with two characteristic frequencies corresponding to a limit cycle of the planar system (10). The intermittent excitation of the oscillating mode alternating with periods of roughly steady behavior predicted to exist close to line $Q$ is evident.

With the introduction of differential convection, i.e., when $v_1\neq v_2$, the codimension-2 singularity is traced numerically using (9) and (4). We have the additional parameter $v$, so that the singularity will be now in general a surface in the four-dimensional parameter space $(a,b,\delta,v)$. The surface can be traced, for example, with lines on which $\delta$ is constant. Projections of a few of these curves on the $a$-$\delta$ plane are shown as solid lines in Fig. 7. The lines extend from the Turing-Hopf line Γ (dotted line) up to a point where the singularity ceases to exist. This is due to the scenario sketched in Fig. 1, when the two critical wave numbers converge as $v$ increases until they meet at a point in which the growth rate becomes "single peaked." Figure 8 shows the critical wave numbers $k_A$ and $k_B$ as a function of differential velocity along

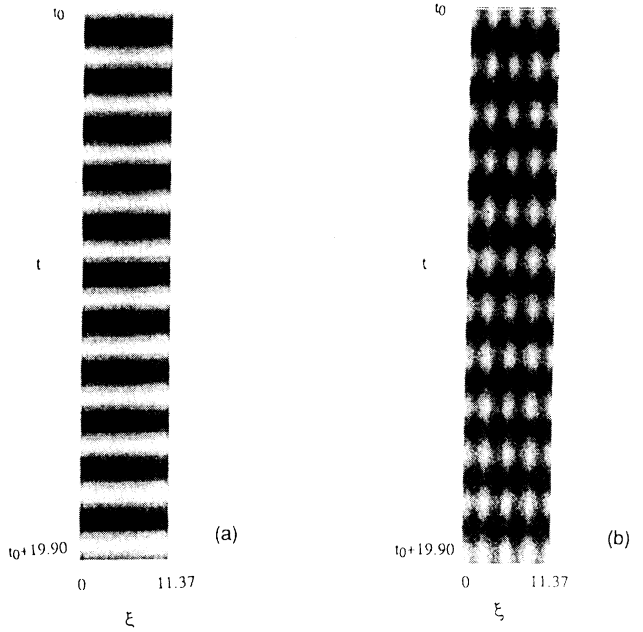


FIG. 5. Activator concentration $c_1(\xi,t)$ resulting from numerical simulations for the Brusselator model. The values of the parameters correspond to point A ($a=3.59$, $b=13.89$, $\delta=0.5776$, $v=0$) and B ($a=3.59$, $b=13.897$, $\delta=0.5776$, $v=0$) in Fig. 4 for (a) and (b), respectively. In the grey scale patterns, darker scales correspond to higher activator concentration. The system tends to homogeneous oscillations for point A and to a mixed mode for point B.

a few of these singular lines with constant $\delta$. The behavior is evidently consistent with our asymptotic analysis in Sec. II predicting for small $v$ a linear increase and a quadratic decrease, respectively, for the long and short critical wave numbers $k_A$ and $k_B$ with increasing differential velocity.

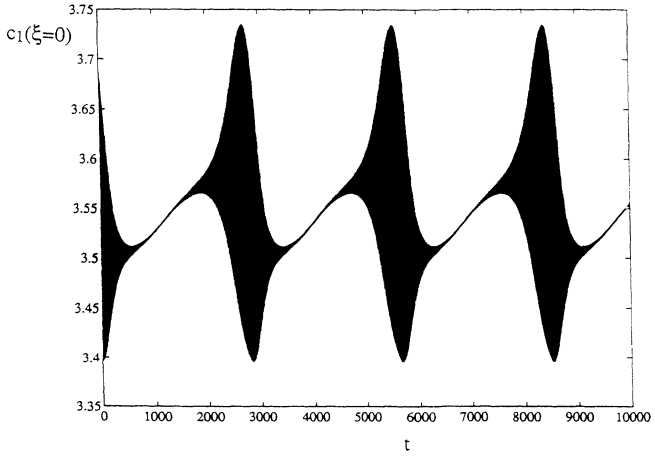


FIG. 6. Activator concentration at the left boundary ($\xi=0$) of the reactor as a function of time from numerical simulation for the Brusselator model with parameters corresponding to point C in Fig. 4 ($a=3.59$, $b=13.8981$, $\delta=0.5776$, $v=0$). A two-torus corresponding to a periodic orbit for the planar system (10) is approached (the fast oscillations cannot be distinguished in the resolution of the graph).

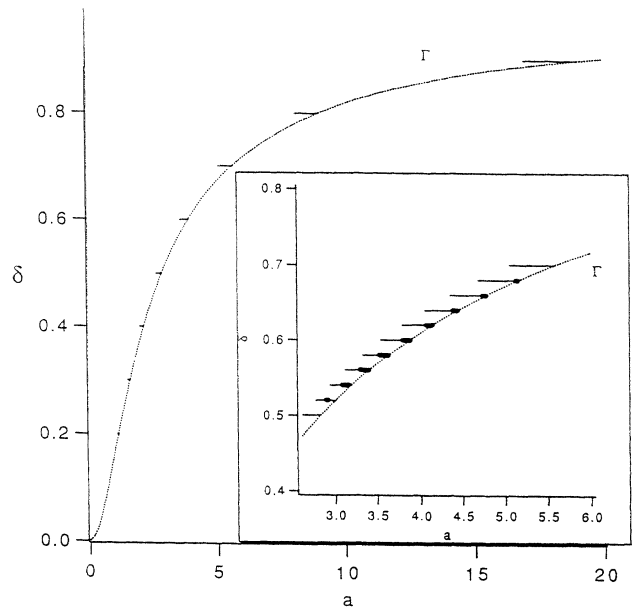


FIG. 7. Lines with constant $\delta$ spanning the surface locus of codimension-2 singularities for $v\neq 0$ extend from the Hopf-Turing line $\Gamma$ to a point at which the two critical wave numbers $k_A$ and $k_B$ merge. In the inset, points on the lines in which case VIa is the predicted unfolding are shown as solid circles.

For the points on the lines spanning the singular surface, the normal form coefficients have been computed and the region in which case VIa is the predicted unfolding is extended, as shown by circles in the inset in Fig. 7. In Fig. 9 the unfolding around a particular point of this region is shown. Unlike the previous case, the transport

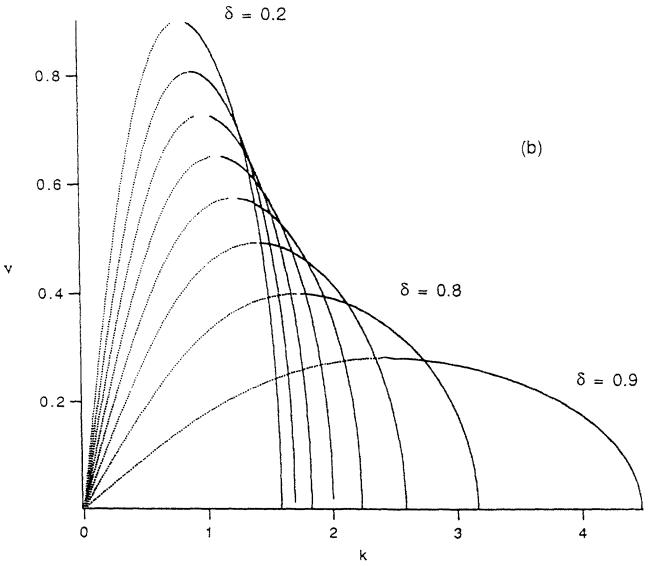


FIG. 8. The critical wave numbers $k_A$ (dotted lines) and $k_B$ (solid lines) along the singular lines for fixed $\delta$ converge towards each other as $v$ increases. The linear increase of $k_A$ and quadratic decrease of $k_B$ with small differential velocity predicted by the asymptotic analysis are evident.

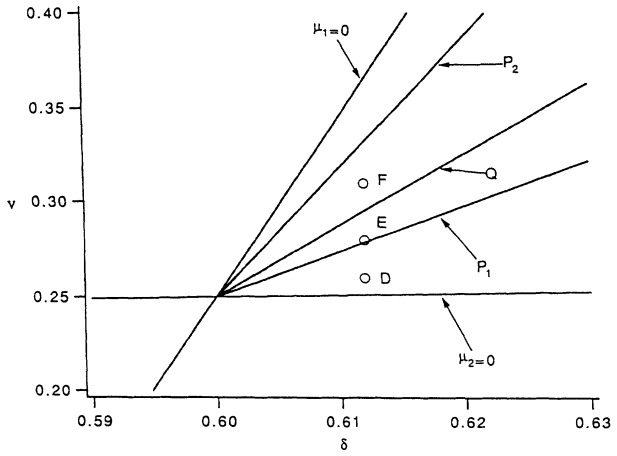


FIG. 9. The unfolding of the double-Hopf singularity with $\delta=0.612$, $v=0.25$, $a=3.815\,394$, and $b=15.410\,747$ in the $\delta,v$ plane. The points denoted with circles are the ones for which numerical simulation results are shown in Figs. 10–12.

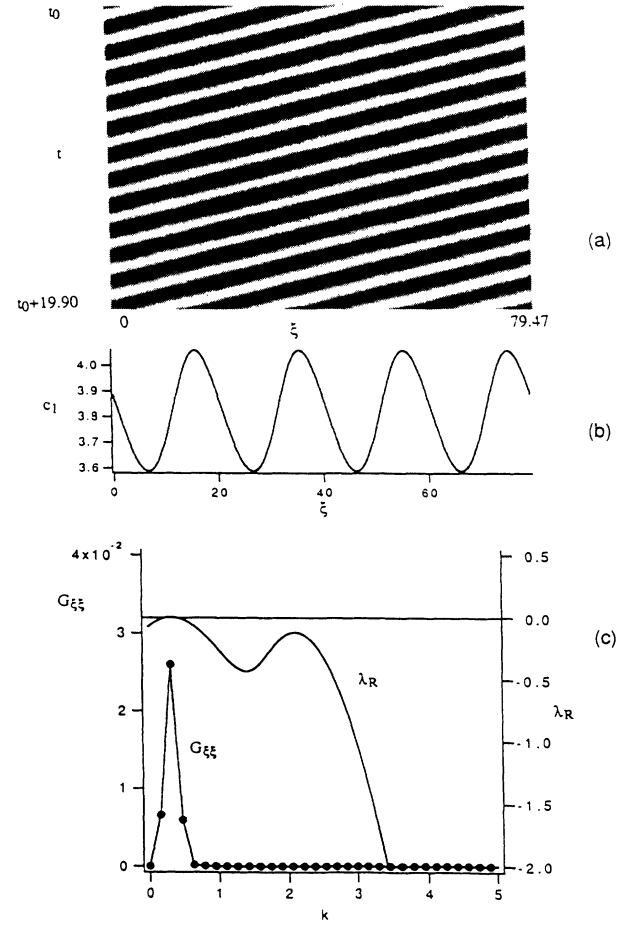


FIG. 10. Activator concentration $c_1(\xi,t)$ from numerical simulations for the Brusselator model with parameters corresponding to point D in Fig. 9 ($a=3.815\,394$, $b=15.410\,747$, $\delta=0.612$, $v=0.26$). (a) Space-time pattern in which darker scales correspond to higher activator concentration, (b) a snapshot, and (c) its spatial Fourier spectrum $G_{\xi\xi}$ compared to the linear growth rate. The system approaches a finite-amplitude traveling wave arising from the convective mode.

parameters $\delta$ and $v$ have been used here as unfolding parameters. The following scenario is hence predicted by the analysis in this case in which differential convection is present. Line $\mu_2=0$ represents the linear stability boundary above which a long traveling wave due to the convective instability appears. Line $P_1$ represents the transition from a finite-amplitude long traveling wave to a mixed mode with two characteristic frequencies obtained by superposition of two different traveling waves, a long one due to the convective instability and a short one due to the Turing instability. The line $Q$ in this case represents transition to a family of three-tori and the correspondent of the heteroclinic orbit for the planar system (10), around which we expect more complex spatiotemporal behavior. Again, simulations show good agreement with such predictions. In this case the simulations of (1) are carried out with $v_1=v$, $v_2=0$, and periodic boundary conditions to allow traveling waves on a domain which is large enough to contain a few wavelengths of the long-wave critical mode. The transition from pure mode to mixed mode can be seen in Figs. 10 and 11 where results of simulations for parameters corresponding to points D and E in Fig. 9, respectively, are reproduced. A spatial

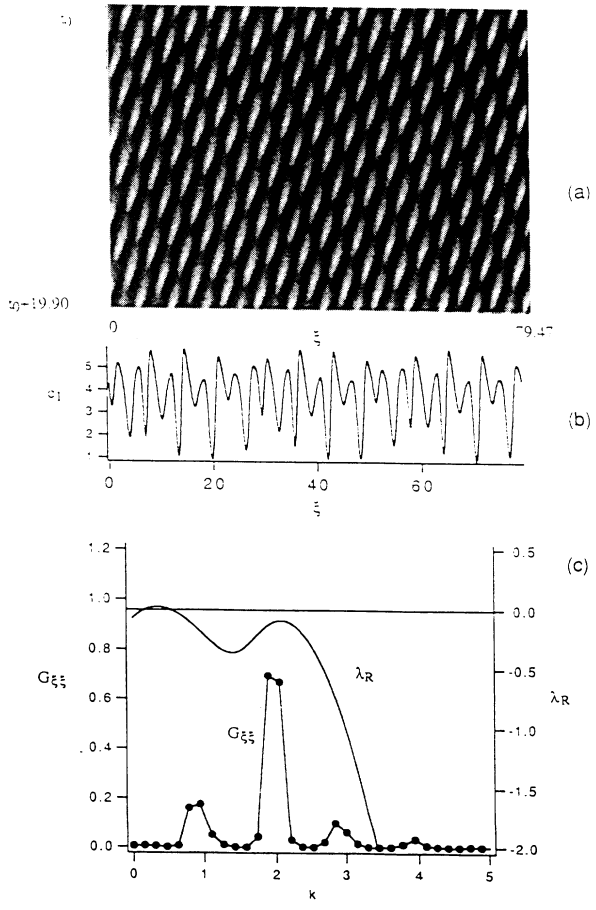


FIG. 11. Same as Fig. 10, but with parameters corresponding to point E in Fig. 9 ($a=3.815\,394$, $b=15.410\,747$, $\delta=0.612$, $v=0.28$). The system approaches a mixed mode with two characteristic wavelengths.

Fourier transform of a snapshot shows the dominant contribution of the modes kept in the discrete-mode model and is compared with the linear growth rate in Figs. 10(c) and 11(c). The "subcritical" transition to a pattern dominated by a single mode (the modified Turing one) which is linearly stable is evident in Fig. 11. Harmonics and the subharmonic of the Turing mode are also present. But the most interesting dynamic behavior is the one observed close to line $Q$, where complex transients exhibit coexisting patches of different monochromatic waves. Simulations in a larger domain for these conditions show how the presence of long-wave modulations in the convective traveling wave mode causes the local amplitude to exceed the average value at certain localized positions, triggering the dramatic "subcritical" transition to the mixed mode in spatially localized fashion (Fig. 12).

As an additional example, we examined the possibility of interactions of multiple instabilities in a more realistic kinetic model. The Belousov-Zhabotinskii reaction is one of the most studied reactions giving rise to exotic behavior [17]. Chemical oscillations, Turing structures, chaotic patterns [18], and differential-flow-induced traveling waves [4] have been separately observed or predicted to exist in the system. A few low-dimensional simplified kinetic models have been proposed over the years and shown to reproduce qualitatively most of the behavior observed experimentally. We report partial results of our analysis performed on one of these models, the two-variable Oregonator [19], for which

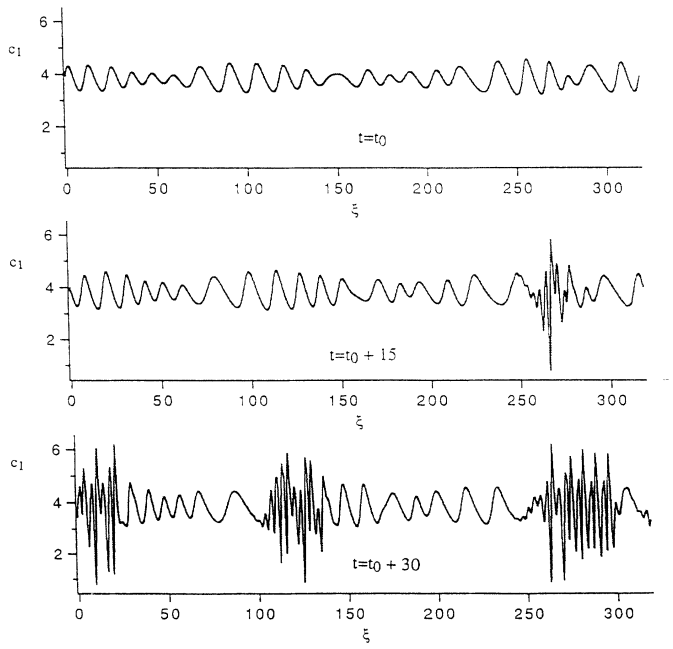


FIG. 12. Numerical simulation results for the Brusselator model with parameters corresponding to point F in Fig. 9 ($a=3.815\,394$, $b=15.410\,747$, $\delta=0.612$, $v=0.31$). The three snapshots, separated by $\Delta t=15$, show how long-wave modulation of the convective mode yields a transition to the short-wave mode which is localized in space.

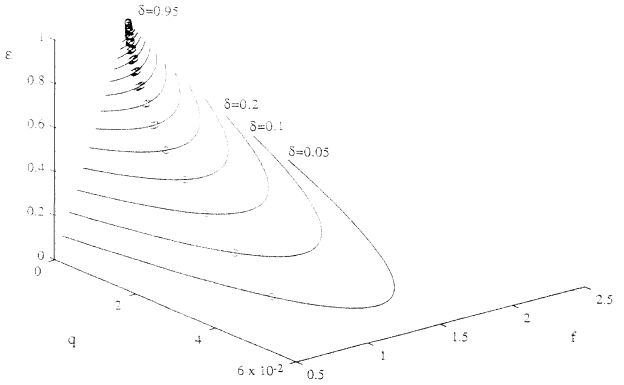


FIG. 13. Lines with constant $\delta$ spanning the Hopf-Turing singularity surface for the Oregonator model (13). The open circles denote points in which the normal form analysis predicts unfolding scenarios of case VIa.

$$f_1(c_1,c_2)=\frac{1}{\epsilon}\left[c_1(1-c_1)+fc_2\frac{q-c_1}{q+c_1}\right],$$
$$f_2(c_1,c_2)=c_1-c_2\ . \tag{13}$$

In the absence of differential velocity, the locus of $(0,\pm i\omega_0)$ points is a surface in the three-dimensional kinetic parameter space ($\mathbf{r}=[f,q,\epsilon]$) which was located numerically. Lines with constant ratio of diffusivities $\delta$ spanning this surface are shown in Fig. 13. Along these lines, the normal form coefficients were computed. The results indicate that there is also the possibility of interesting spatiotemporal behavior in this more realistic model. Points in the parameter space in which case VIa is the predicted unfolding are outlined as circles in Fig. 13. Even for all these points, the analysis predicts interaction between supercritical homogenous kinetic oscillations and a subcritical Turing mode, so that the predicted behavior for the full system(1) is qualitatively the same as the one depicted in Figs. 5 and 6 for the Brusselator. With the introduction of a small differential convective velocity, the complex behavior of Figs. 10–12 is also expected to appear for this model.

## V. DISCUSSION

A difference $\Delta v$ is convection velocities for an activator-inhibitor pair can trigger a traveling wave mode whose characteristic wave number scales as the differential velocity for small $\Delta v$. In fact, as Rovinsky and Menzinger have shown, differential convection can be exploited to induce inhomogeneous patterns in systems in which the formation of Turing patterns is not possible. For large enough differential velocities, the effect of the two destabilizing differential-transport mechanisms is undistinguishable, yielding only a maximum in the growth rate. However, we have shown here that for low differential convection $\Delta v^2/KD_2 \ll 1$, the long-wave convective mode is distinct from the short-wave Turing mode arising from differential diffusion as the growth rate exhibits the distinctive double humps. The nonlinear interaction of the instabilities was shown to produce exotic

nonlinear dynamics in an open-flow reactor, not unlike the long-short wave interactions found in hydrodynamical systems. This is quite exciting since a two-species homogeneous kinetics cannot exhibit temporal chaos because a two-dimensional dynamical system cannot contain a chaotic attractor. Allowing for spatial gradients, diffusion can induce complex behavior through the phase turbulence mechanism [11]. With activator-inhibitor kinetics, additional routes to complexity are possible. For example, the previously studied [9] Hopf-Turing interaction, a limiting case of our analysis, can also give rise to interesting spatiotemporal dynamics such as the mixed mode shown in Fig. 5. However, in both the phase turbulence and the Hopf-Turing scenarios, the homogeneous linear instability, which occurs in a well-mixed reactor, plays a major role and was indeed found to be necessary for Turing-Hopf interaction in the two kinetic models we studied. This is not the case for the complex behavior due to the long-short wave interaction proposed here between modes induced by differential convection and differential diffusion. The spatiotemporal dynamics of the distributed system in this case can be very complex and is independent from the existence of oscillations in the well-mixed system.

The less restrictive conditions for its existence [3] and the immediate success [4] in obtaining its experimental confirmation suggest that the instability due to differential convection is more commonly encountered than the classical Turing one. Even if the latter mode is stable, our analysis shows that complex patterns can still be triggered by interaction between the unstable convective instability and the stable Turing mode. The differences in transport coefficients necessary in order for these modes to be excited are ubiquitous in multiphase systems. One hence expects complex spatiotemporal patterns to be quite common in heterogeneous open-flow reactors. This is consistent with the large amount of data in the literature on irregular thermal patterns exhibited by highly exothermic oxidation reactions. In such systems, the autocatalytic activator variable is the temperature and the inhibitor a reactant. These systems are known to exhibit homogeneous oscillations, and one simply needs a difference in the effective mass and thermal convection or an appropriate Lewis number to obtain the nonhomogeneous patterns.

The patterns due to the long-short wave interaction uncovered here can be rendered even more complex if the Kuramoto phase turbulence due to streamwise sideband instabilities and the subharmonic instability can also be triggered under conditions further from criticality. When the differential velocity is zero, the Turing mode at $k_T$ is a static one and the classical Eckhaus bound stipulates that the critical mode is stable to sideband disturbances. However, the homogeneous kinetic mode at $k=0$, the convective mode at $k_A$, and the modified Turing mode at $k_B$ are all oscillatory modes. The phase instability criterion [11] for these dispersive modes can easily be satisfied and phase turbulence can occur. The subharmonic instability can also occur sufficiently far from criticality [12], leading to more complex dynamics, and we see some evidence of it within our numerical simulations. The long-short wave instability studied here, the sideband instability, and the subharmonic instability are expected to be the dominant instabilities in a one-dimensional open-flow reactor whose cross-stream dimensions are small relative to the reactor length. They represent how extra degrees of freedom due to the spatial variation induced by finite convection and diffusion rates in a large domain can introduce rich spatiotemporal dynamics to rather simple chemical reactions.

## ACKNOWLEDGMENT

This work is supported by NSF Grants No. CTS91-12977 and No. CTS92-00210.

[1] A. M. Turing, Philos. Trans. R. Soc. London, Ser. B **237**, 37 (1952).
[2] V. Castets *et al.*, Phys. Rev. Lett. **64**, 2953 (1990).
[3] A. B. Rovinsky and M. Menzinger, Phys. Rev. Lett. **69**, 1193 (1992).
[4] A. B. Rovinsky and M. Menzinger, Phys. Rev. Lett. **70**, 778 (1993).
[5] S. L. Lane and D. Luss, Phys. Rev. Lett. **70**, 830 (1993).
[6] G. Ertl, Science **254**, 1750 (1991).
[7] C.-C. Chen, E. E. Wolf, and H.-C. Chang, J. Phys. Chem. **97**, 1055 (1993).
[8] J. Guckenheimer, in *Dynamical Systems and Turbulence,* edited by D. A. Rand and L. S. Young (Springer-Verlag, New York, 1981), p. 99.
[9] A. B. Rovinsky and M. Menzinger, Phys. Rev. A **46**, 6315 (1992).
[10] M. Cheng and H.-C. Chang, Phys. Fluids A **2**, 1364 (1990).
[11] Y. Kuramoto, *Chemical Oscillations, Waves, and Turbulence* (Springer-Verlag, Berlin, 1984).
[12] M. Cheng and H.-C. Chang, Phys. Fluids A **4**, 505 (1992).
[13] M. Sangalli, Ph.D. thesis, University of Notre Dame.
[14] J. Guckenheimer and P. Holmes, *Nonlinear Oscillations, Dynamical Systems, and Bifurcations of Vector Fields* (Springer-Verlag, New York, 1983).
[15] S. Wiggins, *Global Bifurcations and Chaos* (Springer-Verlag, New York, 1988).
[16] G. Nicolis and I. Prigogine, *Self-Organization in Nonequilibrium Systems* (Wiley, New York, 1977).
[17] S. K. Scott, *Chemical Chaos* (Oxford University Press, Oxford, 1991).
[18] A. B. Rovinsky, J. Phys. Chem. **91**, 5113 (1987).
[19] J. J. Tyson, Ann. N.Y. Acad. Sci. **316**, 279 (1979).

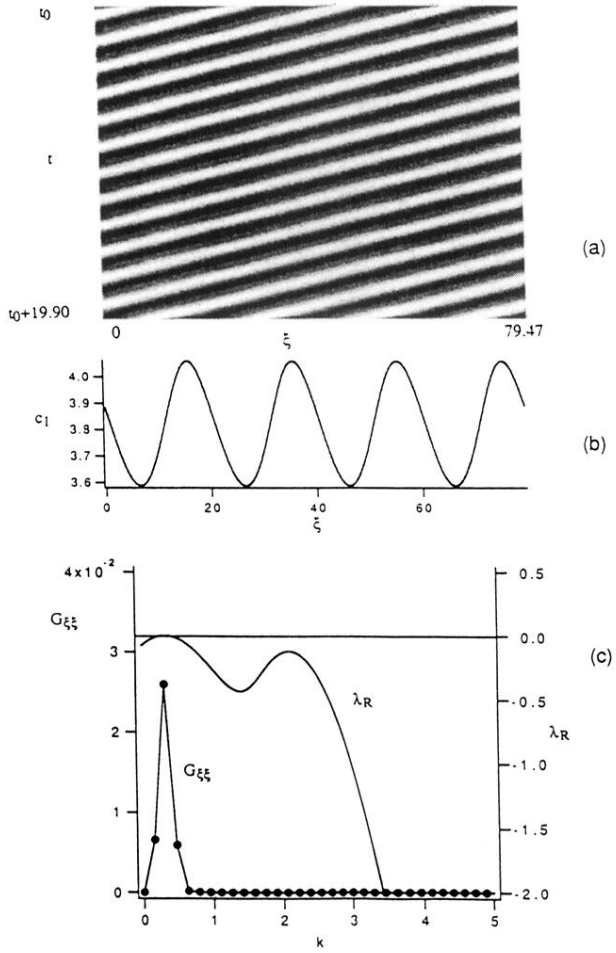


FIG. 10. Activator concentration $c_1(\xi,t)$ from numerical simulations for the Brusselator model with parameters corresponding to point D in Fig. 9 ($a=3.815\,394$, $b=15.410\,747$, $\delta=0.612$, $v=0.26$). (a) Space-time pattern in which darker scales correspond to higher activator concentration, (b) a snapshot, and (c) its spatial Fourier spectrum $G_{\xi\xi}$ compared to the linear growth rate. The system approaches a finite-amplitude traveling wave arising from the convective mode.

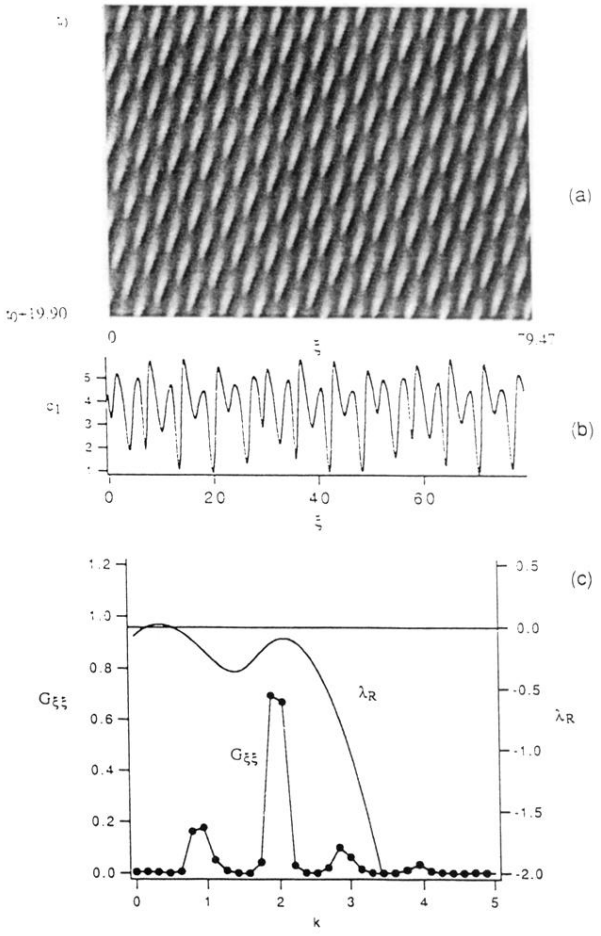


FIG. 11. Same as Fig. 10, but with parameters corresponding to point E in Fig. 9 ($a=3.815\,394$, $b=15.410\,747$, $\delta=0.612$, $v=0.28$). The system approaches a mixed mode with two characteristic wavelengths.

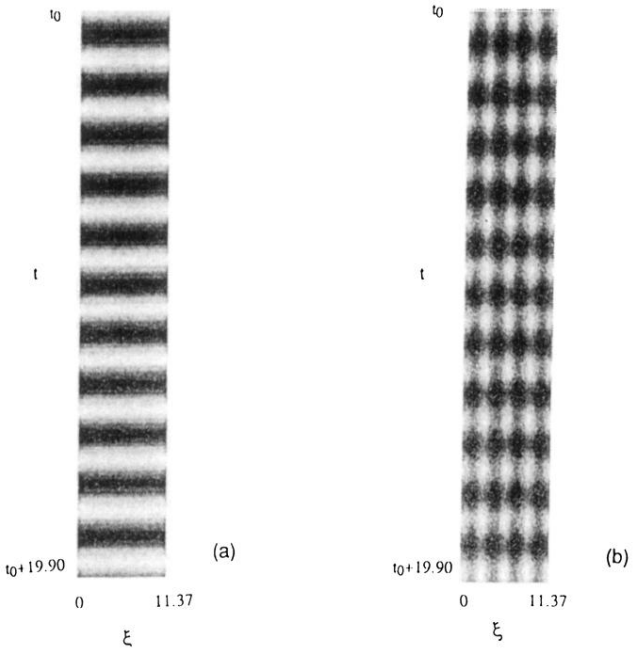


FIG. 5. Activator concentration $c_1(\xi,t)$ resulting from numerical simulations for the Brusselator model. The values of the parameters correspond to point A ($a=3.59$, $b=13.89$, $\delta=0.5776$, $v=0$) and B ($a=3.59$, $b=13.897$, $\delta=0.5776$, $v=0$) in Fig. 4 for (a) and (b), respectively. In the grey scale patterns, darker scales correspond to higher activator concentration. The system tends to homogeneous oscillations for point A and to a mixed mode for point B.